Monte Carlo theory of optical dephasing in LaF_3:Pr^{3+}

R. G. DeVoe, A. Wokaun,* S. C. Rand,† and R. G. Brewer
IBM Research Laboratory, San Jose, California 95193
(Received 31 October 1980)

Recent optical free-induction-decay (FID) measurements of the impurity ion Pr^{3+} in LaF_3 at 2 °K reveal optical homogeneous linewidths of only a few kilohertz, considerably narrower than the inhomogeneous broadening due to crystalline strains (5 GHz) or the static local magnetic fields of the ^{19}F nuclei (100 kHz). In this regime, the homogeneous broadening arises from local field fluctuations, as in NMR, and is due to the ^{19}F nuclei which undergo resonant flip-flops and modulate the Pr^{3+} optical transition frequency. We treat the optical response of a two-level quantum system to an intense coherent field and to fluctuating perturbations using a Monte Carlo computer routine that assumes (1) the LaF_3 crystal structure and (2) a sudden fluorine spin-flip model. This procedure avoids many of the approximations of previous analytic theories of spectral diffusion in magnetic resonance and extends the calculation specifically to optical FID. The decay behavior is obtained by sampling statistically the Pr^{3+} phase history as subgroups of ^{19}F spins flip randomly in space and time. These fluctuations modify the Bloch equations where the solutions for the preparative and post-preparative periods are obtained by numerical integration. In spite of the large lattice size assumed (2250 fluorines), only a few ^{19}F spins contribute substantially to the homogeneous width, a result which shows for the first time that spin-flip correlations are not significant. Furthermore, a Pr^{3+} ion polarizes and detunes the nearest fluorines forming a *frozen core* that is incapable of resonant spin flipping with the bulk fluorines. We demonstrate that the core grows radially as the $^{141}Pr(I=\frac{5}{2})$ magnetic moment increases with I_z, but the Pr optical linewidth changes little, producing essentially one rather than three linewidths. Our calculations utilize no free parameters and predict a Lorentzian line shape of 8.4 kHz half-width at half maximum which compares to the optical FID observation of a 10.1-kHz Lorentzian. The Monte Carlo algorithm is verified further by the static local magnetic broadening of a Pr quadrupole transition which is found to be Gaussian, 82 kHz full width at half maximum, in agreement with a second-moment calculation and current observations.

I. INTRODUCTION

Optical free-induction-decay (FID) measurements have been performed recently on the praseodymium impurity ion Pr^{3+} in a lanthanum trifluoride host crystal LaF_3 at 2 °K yielding a Lorentzian homogeneous linewidth of a few kilohertz—the narrowest optical transition yet observed in a solid.[1,2] Local magnetic dipolar interactions, both homonuclear ^{19}F-^{19}F and heteronuclear ^{141}Pr-^{19}F, are responsible for broadening the line in a way which is reminiscent of past magnetic resonance studies. The optical problem, however, is not identical to previous work because the optical FID effect involves steady state rather than pulse preparation and because optical transitions are usually dominated by inhomogeneous broadening. In this article, we present an optical line-broadening theory involving no free parameters that is suitable for describing the current LaF_3:Pr^{3+} FID observations. The calculation utilizes a Monte Carlo technique that avoids some of the assumptions and approximations of past analytic theories in magnetic resonance and furthermore enables us to gain new insight into the dynamic processes occurring in solids.

In optical FID measurements, it is important to realize that a frequency stabilized cw laser beam resonantly excites a two-level quantum transition and thus coherently prepares a *single* homogeneous Pr^{3+} packet under steady-state conditions.[1,2] Hence, a narrow hole of a few kilohertz width is burned into the much broader inhomogeneous line shape which arises from local crystalline Stark fields (width: 5 GHz) and static magnetic fields of the surrounding fluorine nuclei (width: 100 kHz). In addition to the resonantly excited packet, the remaining packets of the inhomogeneous distribution are excited in an off-resonant manner. When the laser frequency is suddenly switched, the Pr^{3+} ions radiate an intense coherent beam of light in the forward direction, the FID signal, where the time dependence is characterized by a fast and a slow regime corresponding to the

off-resonant and resonant preparation.

The two time regimes are actually limiting cases of a general analytic solution[3] of optical FID, derived recently for an inhomogeneously broadened two-level quantum system subject to steady-state preparation and relaxation characterized by the phenomenological population and dipole dephasing times T_1 and T_2. In the short time limit, the FID heterodyne beat signal

$$E_b^2(t) \sim \chi^2 e^{-(\sigma t/2)^2}, \quad t << 2\gamma/\sigma^2 \ , \tag{1.1}$$

is a Gaussian in time with decay rate $\sigma \equiv 2/T_2^*$ and depends linearly on the laser intensity, χ being the Rabi frequency. This signal reflects the off-resonant preparation of an inhomogeneous line shape which is itself Gaussian with linewidth σ. In the long time limit, the FID signal

$$E_b^2(t) \sim \chi^4 e^{-(1/T_2+\beta)t}, \quad t >> 1/\sigma \ , \tag{1.2}$$

is an exponential and depends nonlinearly on the laser intensity, the leading term being χ^4 where $\beta = 1/T_2(1+\chi^2 T_1 T_2)^{1/2}$. This component corresponds to the resonantly excited packet which is a power broadened Lorentzian of angular linewidth $(1/T_2+\beta)$, the homogeneous width, where in the low power limit

$$\lim_{\chi\to 0}\left(\frac{1}{T_2}+\beta\right) \to \frac{2}{T_2} \ . \tag{1.3}$$

The dominant dynamic mechanism contributing to the Pr^{3+} optical dephasing time T_2 is due to the time varying magnetic dipolar interactions where the ^{19}F nuclei undergo resonant flip-flops and impress weak fluctuating magnetic fields on the ^{141}Pr nuclei. The Pr^{3+} optical transition frequency ω is thereby modulated, and as we shall see the low power limit of Eq. (1.2) omitting trivial factors, takes the more fundamental form

$$E_b^2(t) \sim \Phi(t) \equiv \left\langle \left\langle \exp\left[i \int_0^t \delta\omega(t')\,dt' \right] \right\rangle_{\text{time}} \right\rangle_{\text{lattice}} \ , \tag{1.4}$$

where a time average is to be performed due to the Pr^{3+} frequency fluctuations $\delta\omega(t')$ and a spatial average over the fluorine nuclei surrounding a Pr^{3+} ion. The dipolar mechanism is in fact well substantiated by current optical FID studies where magic-angle line narrowing occurs.[2] Thus, when the Pr^{3+}:LaF_3 crystal is irradiated by an appropriate rf field, the ^{19}F nuclei undergo forced precession about an effective field in the rotating frame. The fluctuating ^{19}F-^{19}F dipolar interaction is quenched thereby and the optical linewidth drops from ~10 to ~2 kHz, a behavior which can occur only when the above broadening mechanism prevails.

The central issue is the evaluation of Eq. (1.4), a magnetic resonance problem which has attracted theorists for about 30 years. For the purpose of discussion, assume a model where isolated A spins of a lattice are monitored by magnetic resonance and are frequently but weakly perturbed by the more numerous B spins. The resulting frequency fluctuations $\delta\omega(t)$ of the A spins and thus the phase integral (1.4) should then follow Gaussian statistics. With the assumption that $\delta\omega(t)$ follows the Gaussian distribution

$$P(\delta\omega) = (1/\delta\sqrt{2\pi}) \exp[-\tfrac{1}{2}(\delta\omega/\delta)^2] \ ,$$

Anderson and Weiss[4] and also Kubo[5] showed that Eq. (1.4) reduces to two limiting cases

$$\Phi(t) = \begin{cases} e^{-\delta^2 t^2/2}, & t << \tau_c \qquad (1.5) \\ e^{-\delta^2 \tau_c |t|}, & |t| >> \tau_c \ , \qquad (1.6) \end{cases}$$

where the depth of modulation $\delta = \langle \delta\omega^2 \rangle^{1/2}$ and the correlation time

$$\tau_c = (1/\delta^2) \int_0^\infty \delta\omega(t')\delta\omega(t'+t)\,dt' \ .$$

Thus, the A spin resonance line exhibits a Gaussian behavior for short times and an exponential decay for long times. As time evolves, the initial linewidth δ narrows to $\delta^2\tau_c$, due either to thermal motion or spin exchange interactions for example. While Eqs. (1.5) and (1.6) superficially resemble the time dependence of the optical problem, Eqs. (1.1) and (1.2), we emphasize that the two theories are unrelated, and as the above discussion indicates, have an entirely different physical origin.

Specific forms for the A spin FID and echo decay were derived initially by Herzog and Hahn[6] using the same model of Gaussian modulation and the Markoff assumption for the correlation function

$$\langle \delta\omega(t)\delta\omega(0) \rangle = \langle \delta\omega(0)^2 \rangle e^{-t/\tau_c} \ .$$

The leading FID terms in the short and long time limit agree with (1.5) and (1.6). Mims[7] also invoked the Gaussian-Markoff model for the time average but included the spatial average of Eq. (1.4) assuming that the dilute A spins are randomly distributed in a lattice of B spins. The resulting echo decay laws are of the form $E(t) = e^{-(2t/T_M)^{3/2}}$ for $t/\tau_c << 1$ and $E(t) = e^{-(2t/T_M)^{1/2}}$ for $t/\tau_c >> 1$ and the FID behavior exhibits similar fractional power laws. This model, therefore, seems inappropriate for optical transients in Pr^{3+}:LaF_3.

Another approach, developed by Klauder and Anderson,[8] assumes a Lorentzian-Markoff model where the abundant B spins execute sudden spin flips randomly in time. The A-B spin dipolar interactions in this case occur less frequently and more violently than the Gaussian modulation described above, and

therefore resemble Poisson statistics[5] which also apply in the line broadening theories of atoms undergoing isolated binary collisions. For a single spin packet, the time and spatial averages, which involve approximations, yield an exponential FID signal of the form

$$F(t) = e^{-mt/R} \ , \tag{1.7}$$

where $m = (8\pi^2/9\sqrt{3})nr\gamma|\mu|$, n is the B spin density, r is the microscopic B spin-flip rate, μ is the B spin moment, and γ is the A spin gyromagnetic ratio. The nature of this model and the resulting exponential decay come closer to explaining the optical FID behavior of Pr^{3+}:LaF_3. However, there is a major difficulty because the parameter R is ill defined for a T_2 process, having been introduced as a device to satisfy stationarity in the Markoffian distribution function.

More recently, Hu and Hartmann[9] obtained analytic results for Eq. (1.4) in the case of the one-pulse FID, the two-pulse echo, and the three-pulse stimulated echo. The system again consists of dilute A spins randomly distributed among the B spins which suddenly and randomly flip between two quantum states because of the spin lattice interaction. The FID signal after a spatial and a time average is given by

$$F(t) = \exp\{-\Delta\omega_{1/2}te^{-Wt}[I_0(Wt) + I_1(Wt)]\} \ , \tag{1.8}$$

and reduces in the short time limit to

$$F(t) = \exp[-\Delta\omega_{1/2}t(1 - \tfrac{1}{2}Wt)], \quad Wt << 1 \ , \tag{1.9}$$

where $\Delta\omega_{1/2} = (16\pi^2/9\sqrt{3})n\mu_A\mu_B/\hbar$, n is the B spin density, μ is a magnetic moment, W is the B spin flip rate, and $I_0(Wt)$ and $I_1(Wt)$ are modified Bessel functions. The leading term $\Delta\omega_{1/2}t$ in Eq. (1.9) is independent of the spin-flip rate W and therefore represents a static magnetic broadening or first order FID, which is unusual in that it is Lorentzian, and follows directly from the spatial average given initially by Mims.[7] The spatial average assumes a continuum behavior in the A-B internuclear spacing, extending from zero to infinity, and therefore is subject to error, an issue considered by Klauder and Anderson,[8] owing to the neglect of the minimum lattice spacing of real crystals. We shall consider the magnitude of this error later in Appendix A. This model also assumes that the entire inhomogeneous line shape is uniformly excited with a $\pi/2$ pulse so that the hole burning preparation which occurs in the optical FID problem is ignored.

The A-B spin dipolar interaction for Pr^{3+}:LaF_3 is neither weak enough to fit a Gaussian theory ($\delta\omega t << 1$), nor strong enough to fit the Klauder-Anderson theory ($\delta\omega t >> 1$). The maximum frequency jump $\delta\omega_{\max}$ due to a fluorine spin flip obeys $\delta\omega_{\max}\tau \sim 1$, where τ is the observed Pr^{3+} dephasing time. Since neither regime applies, a numerical theory is called for.

In this article, a Monte Carlo line broadening theory is presented with the advantage that many of the assumptions and approximations utilized in the past are avoided, and moreover, the role of the dipolar mechanism in the optical FID problem is treated for the first time. We consider a rigid lattice LaF_3 crystal structure[10] which contains a dilute concentration of Pr^{3+} ions. Each Pr^{3+} ion replaces a La^{3+} ion where the Pr^{3+} spatial distribution is random. Second, an external magnetic field is assumed causing the fluorine spins to be either in the up or down orientation. Third, because of a low Pr^{3+} concentration, Pr^{3+}-Pr^{3+} interactions are exluded. Fourth, the F spins are assumed to flip suddenly and randomly at a rate W, a quantity which can be calculated from other considerations and compared with experiment. At low temperatures ($T \leq 2\,^\circ K$), spin-lattice relaxation will not induce fluorine spin flips at a significant rate, but fluorine spin pairs can undergo mutual spin flips as described in Eq. (2.4). In Sec. II, the Pr^{3+} equations of motion are developed in terms of the basic optical field-atom interaction and spin-spin interactions. An expression resembling Eq. (1.4) follows for the Pr^{3+} FID signal in the case of coherent preparation by a monochromatic laser field. In Sec. III, the details of the Monte Carlo calculation are discussed. This step includes the preparation and the sampling procedure for averaging Pr^{3+} phase histories resulting from different fluorine spin distributions. In Sec. IV, the results of the calculations are described. Thus, the static magnetic inhomogeneous broadening calculation is tested by comparing it to a second-moment calculation. For the homogeneous broadening, the nature of a polarized or frozen fluorine core surrounding a local Pr^{3+} ion is analyzed and the dependence of the linewidth on the ^{141}Pr magnetic quantum number is considered.

II. THEORETICAL MODEL

A. Hamiltonian

We seek a solution of the density matrix equations of motion

$$i\hbar\frac{\partial\rho}{\partial t} = [\mathcal{H}, \rho] + \cdots \ , \tag{2.1}$$

where the three dots represent damping terms, for the magnetically perturbed Pr^{3+} ions when they are coherently prepared by a laser field and then experience optical FID.

The Hamiltonian

$$\mathcal{H} = \mathcal{H}^F + \mathcal{H}^{Pr} \ , \tag{2.2}$$

contains terms involving either the ^{19}F nuclear spin S or the $^{141}Pr^{3+}$ ion with nuclear spin I. Thus, the fluorine component

$$\mathcal{H}^{F}=\mathcal{H}_{z}^{F}+\mathcal{H}_{F\text{-}F} \ , \tag{2.3}$$

consists of a Zeeman interaction

$$\mathcal{H}_{z}^{F}=-\gamma_S\hbar\vec{B}\cdot\vec{S} \ ,$$

the external static magnetic field being B, and a homonuclear magnetic dipolar F-F interaction,[11] the secular part being

$$\mathcal{H}_{F\text{-}F}=-\gamma_S^2\hbar\sum_{k<j}\frac{3\cos^2\theta_{kj}-1}{r_{kj}^3} \times[S_{kz}S_{jz}-\tfrac{1}{4}(S_k^+S_j^-+S_k^-S_j^+)] \ . \tag{2.4}$$

The fluorine raising and lowering operators $S_k^{\pm}S_j^{\mp}$ reveal the mutual F-F spin flips which generate local fluctuating magnetic fields that shift the Pr^{3+} transition frequency and broaden the optical transition.

The Pr terms

$$\mathcal{H}^{Pr}=\mathcal{H}_{e}^{Pr}+\mathcal{H}_{Q}^{Pr}+\mathcal{H}_{z}^{Pr}+\mathcal{H}_{Pr\text{-}F}+\mathcal{H}_{0}^{Pr} \ , \tag{2.5}$$

include an electronic component H_e^{Pr}, a quadrupolar term,[12] since $I=\frac{5}{2}$,

$$\mathcal{H}_{Q}^{Pr}=D(I_z^2-\tfrac{1}{3}I^2)+\tfrac{1}{2}E(I_+^2+I_-^2) \ ,$$

a Zeeman term

$$\mathcal{H}_{z}^{Pr}=-\vec{I}\cdot\gamma\cdot\vec{B}\hbar \ ,$$

and the secular part of the Pr-F heteronuclear dipolar interaction of a Pr^{3+} ion with the k surrounding F nuclei of the crystal,

$$\mathcal{H}_{Pr\text{-}F}=-\gamma_1\gamma_S\hbar\sum_{k}\frac{3\cos^2\theta_{kj}-1}{r_{kj}^3}I_zS_{kz}(t) \ . \tag{2.6}$$

Due to the F-F spin flipping, $S_{kz}(t)$ in Eq. (2.6) fluctuates in time and wobbles the Pr^{3+} optical transition frequency.

Because of the assumption of a rigid lattice, we neglect certain T_1 processes, i.e., those processes involving phonons or thermal excitation, but not optical spontaneous emission. Furthermore, because the Pr^{3+} ions are dilute, we ignore secular terms such as $I_{kz}I_{jz}$ arising from the dipolar interaction. Finally, in Eq. (2.6) the flip-flop terms I^+S^- are omitted because the Larmor frequencies of ^{141}Pr and ^{19}F are so different ($\gamma_1 >> \gamma_S$).

The last term of Eq. (2.5) expresses the resonant excitation of a Pr^{3+} ion from its lower state $|1\rangle$ to an upper state $|2\rangle$ by a light wave

$$\vec{E}_x(z,t)=\vec{e}_xE_0\cos(\Omega t-kz) \ ,$$

which induces an electric-dipole transition where

$$\mathcal{H}_{0}^{Pr}=-\vec{\mu}\cdot\vec{E}_x(z,t) \ ,$$

and $\vec{x}$ and $\vec{z}$ are the polarization and propagation directions.

Because $\mathcal{H}_z^F$ commutes with ρ in Eq. (2.1),

$$[\mathcal{H}_z^F,\rho]=0 \ ,$$

Eq. (2.1) reduces to

$$i\hbar\frac{\partial\rho}{\partial t}=[\mathcal{H}^{Pr},\rho]+\cdots \ , \tag{2.7}$$

where the three dots represent damping terms.

B. Optical free induction decay

The time-dependent equations of motion (2.7) now become

$$\dot{\tilde{\rho}}_{12}=\{-\gamma+i[\Delta+\delta\omega(t)]\}\tilde{\rho}_{12}+\tfrac{1}{2}i\chi(\rho_{22}-\rho_{11}) \ , \tag{2.8a}$$

$$\dot{\rho}_{22}-\dot{\rho}_{11}=-\gamma_2\rho_{22}+\gamma_1(\rho_{11}-\rho_{11}^0)+i\chi(\tilde{\rho}_{12}-\tilde{\rho}_{21}) \ , \tag{2.8b}$$

using the definition

$$\rho_{12}(t)\equiv\tilde{\rho}_{12}(t)e^{i(\Omega t-kz)} \ ,$$

and neglecting nonresonant terms. Here, the Rabi frequency χ, the tuning parameter Δ, and the Pr^{3+} eigenenergies in the absence of a light wave are given by

$$\chi=\mu_{12}E_0/\hbar, \quad \Delta=-\Omega+\alpha+\omega_{21}, \quad E_i=\hbar\omega_i(i=1,2) \ ,$$

where α is the shift in the Pr^{3+} transition frequency ω_{21} due to an inhomogeneity in the local static magnetic or crystalline Stark fields.

Fluctuations in the Pr^{3+} transition frequency ω_{21} due to F-F mutual spin flips are included in Eq. (2.8a) through the term

$$\delta\omega(t)=-(\gamma_l'-\gamma_l'')\gamma_S\hbar\sum_{k}\frac{3\cos^2\theta_k-1}{r_k^3}I_zS_{kz}(t) \ , \tag{2.9}$$

which follows directly from Eq. (2.6). Notice that $\delta\omega$ vanishes when the Pr^{3+} gyromagnetic ratio γ_1 of the upper (single prime) and lower (double prime) states are equal.

In Eq. (2.8a), the off-diagonal decay parameter $\gamma\equiv\frac{1}{2}(\gamma_1+\gamma_2)$ consists of the population decay rates γ_1 and γ_2 of states $|1\rangle$ and $|2\rangle$ while the total de-

phasing rate

$$\Gamma \equiv \frac{1}{T_2} = \tfrac{1}{2}(\gamma_1 + \gamma_2) + \gamma_\phi \ , \tag{2.10}$$

includes the contribution γ_ϕ from fluorine spin flips, Eq. (2.9). Note that Eq. (2.10) applies only to that part of the decay which is exponential; it is a convenient expression but not an essential one.

Now assume that a narrow packet from the inhomogeneous line shape is coherently prepared by a cw laser beam under steady-state conditions and that FID follows at time $t=0$ when the laser frequency is switched suddenly by several homogeneous linewidths. The FID solution of Eq. (2.8) takes the form

$$\tilde{\rho}_{12}(t) = \tilde{\rho}_{12}(0) \exp\left[(-\gamma + i\Delta)t + i\int_0^t \delta\omega(t')\,dt'\right] \ , \tag{2.11}$$

where $\tilde{\rho}_{12}(0)$ expresses the coherent preparation at time $t=0$. Equation (2.11) involves the phase history of a single Pr^{3+} ion and therefore must be averaged over the distribution of frequency fluctuations occurring at different Pr^{3+} sites both during the preparative period $t \leq 0$ and afterward $t \geq 0$. In addition, averages are to be performed over the local inhomogeneous static magnetic and crystalline Stark fields. Writing all of these averages symbolically by a single bracket, Eq. (2.11) becomes

$$\langle \tilde{\rho}_{12}(t) \rangle = \left\langle \tilde{\rho}_{12}(0) \exp\left[(-\gamma + i\Delta)t + i\int_0^t \delta\omega(t')\,dt'\right] \right\rangle \ . \tag{2.12}$$

Finally, the FID signal expressed as the field amplitude

$$E_{12}(z,t) = \tilde{E}_{12}(z,t)e^{i(\Omega t - kz)} + \text{c.c.} \tag{2.13}$$

obeys Maxwell's wave equation

$$\frac{\partial \tilde{E}_{12}(t)}{\partial z} = -2\pi i k N \mu_{12} \langle \tilde{\rho}_{12}(t) \rangle \tag{2.14}$$

for an optically thin sample where N is the Pr^{3+} ion density and μ_{12} is the electric-dipole transition matrix element. Because of the laser frequency shift $\Omega - \Omega'$, the FID signal $F(t)$ appears as a heterodyne beat due to the cross terms in the total field intensity, i.e.,

$$F(t) = \tfrac{1}{2} E_0 \tilde{E}_{12}(t) e^{i(\Omega - \Omega')t} + \text{c.c.} \tag{2.15}$$

Thus, the FID signal is determined essentially by the statistical behavior of Eq. (2.12) where the fluctuations $\delta\omega(t)$ introduce an additional damping.

III. MONTE CARLO CALCULATION

Outline and assumptions

We begin by writing the Pr^{3+} density matrix average (2.12) as a sum

$$\langle \tilde{\rho}_{12}(t) \rangle = \frac{1}{N} \sum_{j=1}^{N} \tilde{\rho}_{12}^{j}(0) \times \exp\left[(-\gamma + i\Delta_j)t + i\int_0^t \delta\omega_j(t')\,dt'\right] \ , \tag{3.1}$$

over N different Pr^{3+} environments that arise from the local static and fluctuating fluorine spin configuration and the crystalline Stark fields. The index j, therefore, labels a particular ion's preparation $\tilde{\rho}_{12}^{j}(0)$ by a resonant laser field in the presence of a fluctuating Pr^{3+} level spacing $\delta\omega_j(t)$, a specific Pr^{3+} Stark shift α_j in the tuning parameter Δ_j, and a specific Pr^{3+} phase history

$$\varphi_j(t) = \int_0^t \delta\omega_j(t')\,dt' \tag{3.2}$$

following the preparation. Thus, Eq. (3.1) includes both time and spatial averages. The number of Pr^{3+} ions N must be sufficiently large that fluctuations in $\langle \tilde{\rho}_{12}(t) \rangle$ due to finite sample size are negligible. We shall see that this criterion is satisfied for a model where N is in the range 10^3 to 10^6 even though about 10^{15} Pr^{3+} ions are monitored experimentally.

An outline of the numerical evaluation of Eq. (3.1) is shown schematically in Fig. 1 and yields (1) the dynamic or homogeneous magnetic broadening due to fluctuations $\delta\omega_j(t)$ in the Pr^{3+} level spacing and (2) a static or inhomogeneous magnetic broadening due to the frequency shift $\delta\omega_j(0)$.

The calculation of the random frequency fluctuation $\delta\omega_j(t)$ can be simplified by writing Eq. (2.9)

$$\delta\omega_j(t) = \sum_k \omega_k \frac{S_{kz}^{j}(t)}{|S_{kz}^{j}(t)|} \ , \tag{3.3}$$

in terms of the static frequency shift

$$\omega_k = |\gamma_I' - \gamma_I''| I_z B_k \tag{3.3'}$$

due to the field of the kth fluorine nucleus,

$$B_k = \mu_F \frac{(3\cos^2\theta_k - 1)}{r_k^3} \ . \tag{3.4}$$

Assumption 1. The sudden jump approximation assumes that the fluorine spin $S_{kz}^{j}(t)$ is restricted to two values $+\frac{1}{2}$ or $-\frac{1}{2}$, and that the jump occurs instantaneously between these two values at random times with an average rate $W \equiv 1/T$ where T is the mean time between jumps. The pairwise correlation of spin

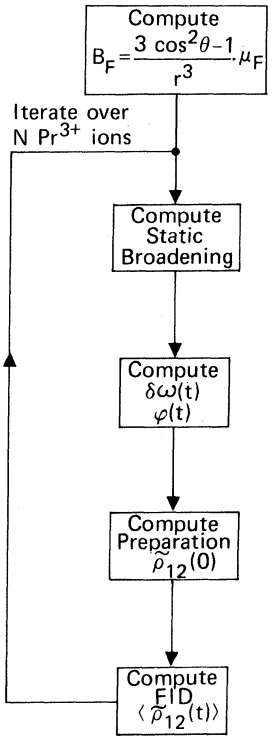

FIG. 1. Schematic diagram of the sequence of operations of the Monte Carlo calculation.

flips implied by Eq. (2.4) is ignored. It is possible to write Eq. (3.3) because the only dependence on t or j in $\delta\omega_j(t)$ lies in $S_{kz}^j(t)$, and, the various frequency histories differ only in the time evolution of the signs of the fluorine fields. The first stage in the Monte Carlo program is the calculation of a table of fluorine magnetic fields B_k using (3.4).

Assumption 2. The angles θ_k and distances r_k of the 2250 fluorines in the nearest 125 unit cells around a Pr site are computed from the LaF_3 crystal structure ($P3C1 - D_{3d}^3$), data of Zalkin, Templeton, and Hopkins.[10]

Assumption 3. The c axis of the LaF_3 crystal is assumed to be parallel to an external magnetic field B_0 (z axis), and B_k represents the z component of the fluorine dipolar field where $\mathcal{H}_Q^{Pr} > \mathcal{H}_z^{Pr} > \mathcal{H}_{Pr\text{-}F}$. The resulting table of field strengths B_k is used in all subsequent calculations.

Assumption 4. For simplicity, we assume only one g value for the ground and one for the excited electronic state of Pr^{3+}, avoiding the complexity of the anisotropic g tensor.

The second stage of the program computes the static magnetic broadening due to a random initial alignment of the fluorine spins $S_{kz}^j(0)$. For each value of j, the fluorine magnetic fields B_k, obtained in the previous step, are summed with a random distribution in their sign. The resulting frequency shift $\delta\omega_j(0)$ is computed using Eq. (3.3) and its distribution function

$$G \equiv \frac{dN}{d(\delta\omega_j(0))} , \tag{3.5}$$

is plotted in Fig. 2.

The third stage computes the frequency histories $\delta\omega_j(t)$ at 400 discrete times t_1 where the fundamental interval $\Delta t \equiv t_{1+1} - t_1$. The time origin $t_0 = 0$ now coincides with the beginning of the preparative period which extends over the initial 200 points ($t_0 \rightarrow t_{200}$) and spans a much longer period than the optical dephasing time. During this period, the laser induces a polarization in the sample which simulates steady-state preparation. The second 200 points ($t_{200} \rightarrow t_{400}$), which we consider later, correspond to the free decay period when the laser is out of resonance with the initially prepared packet.

Assumption 5. To calculate $\delta\omega_j(t)$, we assume that the number of fluorine spin flips per unit time n follows a Poisson distribution in time with a mean value

$$n_0 = N_F W ,$$

where N_F is the number of fluorine nuclei and W is the average spin-flip rate. Next, a subgroup of fluorine spins, $n(t_1)\Delta t$ in number at time t_1, are chosen randomly in space and undergo a spin flip (sign reversal in B_k) producing a field fluctuation at the Pr^{3+} site and a frequency shift $\delta\omega_j(t_1)$. The calculation is repeated 400 times, generating a new shift for each succeeding time interval Δt so that a frequency history evolves where each shift adds to the previous value. Once a value for W is selected, the temporal distribution in spin flips follows a Poisson distribution and the spatial distribution varies randomly from one time interval to another, producing variations in $\delta\omega_j(t_1)$. The phase histories $\phi_j(t_1)$ are

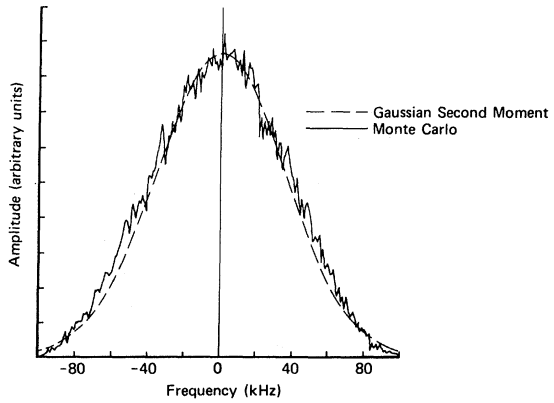

FIG. 2. Magnetic inhomogeneous broadening of a ^{141}Pr quadrupole transition showing the Gaussian line shape of the Monte Carlo calculation (164 kHz FWHM) and an overlapping Gaussian having a width equal to the second moment.

obtained readily from Eq. (3.2).

In the fourth step, the preparation $\tilde{\rho}_{12}^{j}(t_{200})$ is computed by numerically integrating the density matrix Eqs. (2.8) or equivalently the Bloch equations

$$\begin{aligned}\dot{u}_j(t) &= -[\Delta_j + \delta\omega_j(t)]v_j(t) - \gamma u_j(t) \ , \\ \dot{v}_j(t) &= [\Delta_j + \delta\omega_j(t)]u_j(t) + \chi w_j(t) - \gamma v_j(t) \ , \\ \dot{w}_j(t) &= -\chi v_j(t) - [w_j(t) - w^0]/T_1 \ ,\end{aligned} \tag{3.6}$$

where

$$\tilde{\rho}_{12}^{j}(t) = u_j(t) + i v_j(t) \ . \tag{3.7}$$

For simplicity, it is assumed that the population difference w is characterized by the single decay time T_1, and the other parameters are defined in Sec. II B. The initial conditions are $\rho_{11}(t_0) - \rho_{22}(t_0) = 1$, $\tilde{\rho}_{12}(t_0) = 0$, and the preparation is confined to the interval $t_0 \rightarrow t_{200}$.

Finally, the FID signal $\langle \tilde{\rho}_{12}(t) \rangle$ is calculated in Eq. (3.1) by iterating the preceding four steps N times to obtain the average $\langle \tilde{\rho}_{12}^{j}(t) \rangle$ in the post-preparative period $t > t_{200}$. The effect of inhomogeneous broadening is included by allowing the inhomogeneous shift α_j to vary randomly over its line shape.

IV. RESULTS

A. Magnetic inhomogeneous broadening

Due to the $^{141}Pr(I = \frac{5}{2})$ hyperfine structure, the $^3H_4 \leftrightarrow {}^1D_2$ optical transition is expected to consist of three prominent transitions $(I_z'' \rightarrow I_z') = (\frac{1}{2} \rightarrow \frac{1}{2})$, $(\frac{3}{2} \rightarrow \frac{3}{2})$, and $(\frac{5}{2} \rightarrow \frac{5}{2})$, separated from each other by $\sim$10 MHz but overlapping due to the crystal strain broadening of 5 GHz. The Monte Carlo calculations show that these three lines also are broadened inhomogeneously by the fluorine static magnetic fields; the line shapes are given by the distribution function G, Eq. (3.5), and are found to be Gaussian with a full width at half maximum (FWHM) linewidth of $42(I_z = \frac{1}{2})$, $126(\frac{3}{2})$, and $210(\frac{5}{2})$ kHz which are in the ratio of 1:3:5, consistent with Eq. (3.3). These calculations assume that the Pr gyromagnetic ratio $\gamma_I''/2\pi = 11.5$ kHz/G, derived from rf optical double resonance,[13] and that $\gamma_I' \sim 0$ since additional experiments[14] indicate that $|\gamma_I'| \leq \frac{1}{5}|\gamma_I''|$ where the relative sign of the $^1D_2$ and $^3H_4$ splittings are unknown. Erickson has kindly informed us that the above value of γ_I'' corrects a numerical error in his previous publication.[13,19]

Because the strain broadening is about 10^4 times larger than the magnetic inhomogeneous broadening, the latter has never been resolved at optical frequencies. The Monte Carlo calculations can be compared, however, to the Pr ground-state quadrupole transition linewidth, determined either by second moment calculations or by optically detected NMR measurements. Since rf transitions require that $\Delta I_z = \pm 1$, Eq. (3.3) becomes

$$\delta\omega_j(0) = \gamma_I'' \sum_k B_k \frac{S_{kz}^{j}(0)}{|S_{kz}^{j}(0)|} \ . \tag{4.1}$$

A comparison of Eq. (3.3) and Eq. (4.1) reveals that the Pr optical and NMR magnetic inhomogeneous linewidths differ only by a scaling factor and are approximately in the ratio of I_z as indicated in Table I. With the aid of Eq. (4.1), the Monte Carlo line shape function is derived for the NMR case and appears in Fig. 2 as a Gaussian profile.

Let us now compare the Van Vleck[15] method of moments which has been used to calculate the nuclear broadening of EPR lines of dilute paramagnetic crystals[16] or the width of nuclear quadrupole transitions.[11] The second moment

$$\langle (\Delta\omega_I^2)_{IS} \rangle_{\text{av}} = \tfrac{1}{3}\gamma_I''^2 \gamma_S^2 S(S+1)\hbar^2 \sum_k \frac{(1 - 3\cos^2\theta_k)^2}{r_k^6} \ ,$$

for a Pr NMR line implies a linewidth

$$\begin{aligned}\Delta\nu &= \frac{1}{2\pi}(\langle \Delta\omega_I^2 \rangle_{\text{av}})^{1/2} \\ &= \frac{1}{2\pi}\gamma_I''\mu_S \left(\sum_k \frac{(1 - 3\cos^2\theta_k)^2}{r_k^6} \right)^{1/2} \ .\end{aligned} \tag{4.2}$$

The lattice sum in Eq. (4.2) has been evaluated for the nearest 2250 fluorine neighbors and equals 0.0548 Å^{-6}, giving a root second moment linewidth $\Delta\nu = 35.8$ kHz. The FWHM linewidth is $2\sqrt{2\ln 2}$ larger or $\Delta\nu_{\text{FWHM}} = 84.5$ kHz.

Figure 2 compares the Monte Carlo line shape to a Gaussian having a width given by the second moment and the agreement is excellent. Note that there are no adjustable parameters in the comparison except the vertical scale. The Monte Carlo program also calculates a root second moment by

$$(\langle \Delta\omega^2 \rangle_{\text{av}})^{1/2} = \left(\frac{1}{N} \sum_{j=1}^{N} [\delta\omega_j(0)]^2 \right)^{1/2} \ ,$$

giving $\Delta\nu = 34.9$ kHz, only 2.5% lower than the Van Vleck result.

In addition to the nearly exact coincidence with the Van Vleck theory, our calculations are supported also by recent Pr ground-state measurements. A steady-state rf optical double resonance experiment[17] yields 180 ± 10 kHz FWHM for $I_z = \frac{1}{2} \rightarrow \frac{3}{2}$ and 200 ± 10 kHz FWHM for $I_z = \frac{3}{2} \rightarrow \frac{5}{2}$ whereas an optically detected spin echo measurement[18] gives 230 ± 25 kHz FWHM for $I_z = \frac{3}{2} \rightarrow \frac{5}{2}$. These results are about a

TABLE I. Linewidths of ^{141}Pr in LaF_3 due to magnetic inhomogeneous broadening.

Transition	Method	Linewidth FWHM (kHz)
rf($\Delta I_z'' = \pm 1$)	Monte Carlo theory[a]	82
	Van Vleck second moment[a]	84.5
	cw rf-optical double resonance[b]	
	$I_z'' = \frac{1}{2} \rightarrow \frac{3}{2}$	$180 \pm 10^c (\sim 100)^d$
	$I_z'' = \frac{3}{2} \rightarrow \frac{5}{2}$	$200 \pm 10^c (\sim 100)^d$
	Optically detected rf transients[e]	
	$I_z'' = \frac{3}{2} \rightarrow \frac{5}{2}$	230 ± 25^c
optical ($^3H_4 \leftrightarrow {}^1D_2$)	Monte Carlo theory[a]	
	$I_z'' \rightarrow I_z' = \frac{1}{2} \rightarrow \frac{1}{2}$	42
	$I_z'' \rightarrow I_z' = \frac{3}{2} \rightarrow \frac{3}{2}$	126
	$I_z'' \rightarrow I_z' = \frac{5}{2} \rightarrow \frac{5}{2}$	210

[a]This work.
[b]Reference 17.
[c]Earth's magnetic field.
[d]Static external field of ≥ 16 G.
[e]Reference 18.

factor of 2 larger than the calculated value because the measurements were conducted in the absence of an external dc magnetic field. However, Erickson[19] has noted that his ~200-kHz linewidth reduces to ~100 kHz when a static field of 16 G or larger is applied, bringing the observations into good agreement with the Monte Carlo linewidth of 84.5 kHz. The theory of line broadening in zero field is more complicated than the calculation presented here as the nonsecular terms of the dipolar interaction must be included. Such a theory, a second moment calculation, was developed by Abragam and Kambe,[20] leading to a similar static dipolar linewidth reduction, a factor of 2 or 3, as the magnetic field is increased from its zero field value. We should also note that the observed homogeneous linewidth[1] displays a similar reduction when the static applied field exceeds 19 G. The results of this section are summarized in Table I.

We conclude that for static broadening the Monte Carlo result is unambiguous as it agrees accurately with the second moment calculation and existing experiments. Furthermore, since the optical and NMR magnetic inhomogeneous linewidths are related trivially by a scale factor, the ratio of Eqs. (3.3) and (4.1), *the second moment calculation itself accurately predicts the optical linewidth arising from a lattice of static dipoles.*

B. Single packet case

Rather than deal with the full expression (3.1) immediately, it is possible to use a simplified form

$$\langle \tilde{\rho}_{12}(t) \rangle \sim \frac{1}{N} \sum_{j=1}^{N} \cos\phi_j(t) \ , \qquad (4.3)$$

which describes many features of the homogeneous broadening problem. Equation (4.3), in fact, is the starting point of many line broadening theories. This expression neglects the sine terms as discussed in Sec. IV C. The simplest form of preparation is assumed also, namely a single homogeneous packet of a two-level quantum system in a 50:50 superposition state. Thus, inhomogeneous and power broadening are ignored.

The use of Eq. (4.3) is preferred over the full Monte Carlo program when several parameters are to be varied simultaneously, since it executes at least two orders of magnitude faster. The essential features of dephasing in this case have been demonstrated by studying the variation of the FID decay time $1/\gamma_\phi$ as a function of (a) the number of fluorines in the lattice, (b) the fluorine position in the lattice, and (c) the fluorine flip rate W.

Our primary result is that a few nearest-neighbor fluorines dominate the dephasing of the Pr^{3+} ion. Figure 3 shows the optical linewidth of the $I_z = \frac{1}{2}$ state for a spin flip time $T = 50$ μsec as a function of the number of fluorines permitted to flip. The abscissa counts the number of interacting fluorines, with the strongest taken first, so that as $N \rightarrow \infty$, only distant, weakly coupled fluorines remain. Thus, the linewidth of the Pr^{3+} in a lattice in which only the two strongest coupled fluorine nuclei flip is $\frac{2}{3}$ that of the whole lattice result, and when five fluorines flip, the linewidth is almost indistinguishable from that of the full lattice.

This conclusion is suggested again by Fig. 4 which shows the distribution function $dN/d\omega_k$ of static frequency shifts ω_k Eq. (3.3′). As expected, most of the 2250 fluorine nuclei interact weakly with a given Pr^{3+}

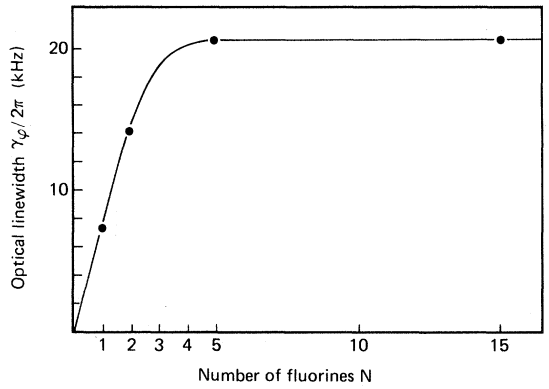

FIG. 3. The Pr^{3+} optical linewidth ($\gamma_\phi/2\pi$ HWHM) of the $^3H_4 \leftrightarrow {}^1D_2$ transition for $I_z = \frac{1}{2}$ and the fluorine spin-flip time $T = 50$ μsec as a function of the number of fluorine nuclei N where the fluorines closest to the ion are plotted first.

ion and produce very small shifts, which we see are in the range 0 to 3 kHz. The largest shifts, which are discrete at 9, 10, and 20 kHz, result from the five nearest-neighbor fluorines which are the main contributors to optical dephasing.

This result has three consequences. *First,* it shows that our lattice size of 2250 fluorines is a few orders of magnitude larger than necessary. *Secondly,* it implies that correlations between adjacent fluorines do not strongly affect the optical linewidth. We do not argue that spin correlations do not exist, but merely that their effect on the linewidth is small since so few fluorine nuclei are involved. The magnetic resonance theories described above[4–9] have not considered the effect of correlations on the linewidth, and no estimate of its effect has previously been given. From Fig. 3, we see that the flipping of one fluorine provides 30% of the linewidth. With two fluorines we reach 67% of the linewidth but this pair is weakly correlated since the crystal structure shows that these fluorines lie on opposite sides of the Pr ion and are about 5 Å apart.

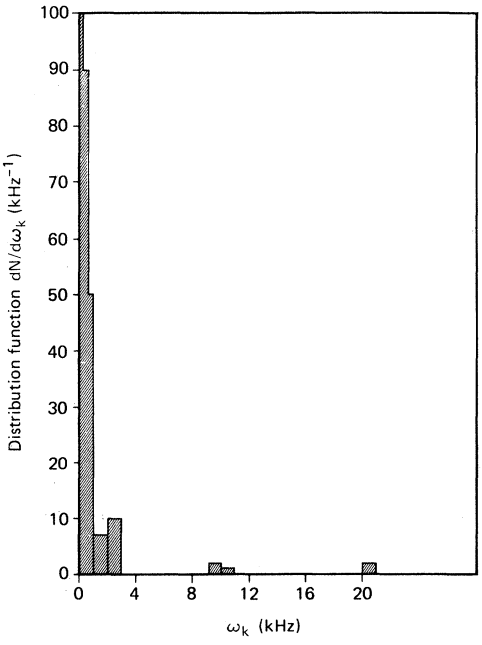

FIG. 4. The Pr^{3+} ion distribution function $dn/d\omega_k$ vs the static frequency shift ω_k.

A physical explanation for the weak correlation lies in the strong radial behavior of the individual fluorine magnetic fields B_k, Eq. (3.4), which are proportional to $1/r^3$. If a nearest-neighbor and a second-nearest-neighbor exchange spin orientation, the second nearest neighbor will produce a shift $(\frac{1}{2})^3$ that of the nearest neighbor, and to current levels of accuracy may be ignored. We note further that the leading role of the nearest neighbors is a familiar concept in the theory of moments[11,15] in NMR, where the second moment is proportional to $\sum 1/r_k^6$.

We have also studied this question further by introducing correlation in a model calculation using five fluorine spins. An extreme form of correlation is assumed where all five spins flip simultaneously. In one case, we assume that the spins are all parallel so that their fields add to produce the largest frequency jump possible. In the second case, a spin orientation is selected which produces the smallest frequency shift. The first correlation increases the linewidth by 35% while the second case decreases it by 20%. Since any physical correlation would be less extreme, we assert that the effect of correlation on the linewidth is less than ±50%.

The *third* consequence of the leading role of the nearest neighbors in optical dephasing is that perturbations of nearby fluorines by the static Pr^{3+} magnetic moment can cause a large reduction in the linewidth. We call this effect the "frozen-core" phenomenon and it has been proposed to explain anomalously narrow linewidths in ESR.[21] The static dipolar magnetic field due to the enhanced nuclear magnetism of the Pr^{3+} ion[22] amounts to several gauss and detunes nearby fluorine nuclei from the resonance frequency established by the external magnetic field. The flip-flop operators $(S_k^+ S_j^- + S_k^- S_j^+)$ in Eq. (2.4) thereby connect states of different energy and for these fluorines spin flips are inhibited. Since those fluorines most strongly coupled to the Pr^{3+} ion are the first to be inhibited, large changes in linewidth result. Furthermore, the three I_z states of Pr^{3+} have different static dipolar fields, in the ratio of 1:3:5. Therefore, the frozen core is "variable," with

a size depending on the Pr^{3+} magnetic substate.

This phenomena has been incorporated into the Monte Carlo routine by modifying Eq. (2.9) to exclude the detuned fluorines:

$$\delta\omega(t) = -(\gamma_I' - \gamma_I'')\gamma_S\hbar \sum_{k \neq k'}^{2250} \frac{3\cos^2\theta_k - 1}{r_k^3} I_z S_{kz}(t) \ .$$

Here $\{k'\}$ represents the lattice indices of the detuned fluorines. A fluorine is included in $\{k'\}$ if its detuning by the Pr ion is greater than the fluorine NMR linewidth of 10 kHz.[23]

In Fig. 5 we plot the optical linewidth with and without a frozen core, as a function of the Pr^{3+} magnetic moment $\mu_z^{Pr} = \gamma_I I_z \hbar$ for $T = 50$ μsec. Without the frozen core, the linewidth is approximately proportional to $|\mu_z^{Pr}|^{1/2}$, in contradiction with our earlier prediction[1,2] that the linewidth should be proportional to $|\gamma_I' - \gamma_I''|$. We note that although the *inhomogeneous* magnetic linewidth (4.1) scales as $|\gamma_I' - \gamma_I''|$, the *homogeneous* linewidth (3.3) does not depend linearly on this factor because of the time dependence of $S_{kz}^I(t)$.

With the frozen core effect included, the homogeneous linewidth is approximately proportional to $|\mu_z^{Pr}|^{1/4}$ for $|\mu_z^{Pr}| \gtrsim 10$ kHz/G. For $|\mu_z^{Pr}| \lesssim 5$ kHz/G the frozen core and no frozen core results are identical, because the radius of the frozen core is less than the nearest-neighbor spacing. Instead of our earlier prediction[1,2] of a triexponential decay with decay rates in the ratio of 1:3:5, Fig. 5 shows a ratio of 1:1.4:1.7. A computer plot of this triexponential decay indicates that it is indistinguishable from a single exponential with a decay rate equal to the average of the $I_z = \frac{1}{2}$, $\frac{3}{2}$, and $\frac{5}{2}$ values. Our experimental observation[24] of a single exponential decay is therefore explained.

Figure 6 shows the dependence of the optical dephasing time $1/\gamma_\phi$ on the mean time T between fluorine flips. Based on the previous discussion, γ_ϕ is the average of the $I_z = \frac{1}{2}$, $\frac{3}{2}$, and $\frac{5}{2}$ decay rates. The quantity T is the only parameter in our theory that is not directly measurable. We shall first treat it as a free parameter and then use an argument of Bloembergen[25] that predicts T from experimental studies of the fluorine NMR linewidth.[23]

First note that for T between 10 and 1000 μsec, the linewidth is within a factor of 2 of the experimental value. To this level of accuracy, then, our results are independent of T. Conventional NMR measurements of the fluorine dephasing time in LaF_3 give a value of $T_2 = 17$ μsec which results from both static and dynamic broadening and does not directly measure the fluorine flip rate. Bloembergen,[25] followed by Lowe and Gade[26] have derived the relationship

$$T \sim 10T_2 \ ,$$

making use of the method of moments to estimate the flip-flop term in $H_{F\text{-}F}$ [Eq. (2.4)] and deriving a transition probability from it. This approach predicts

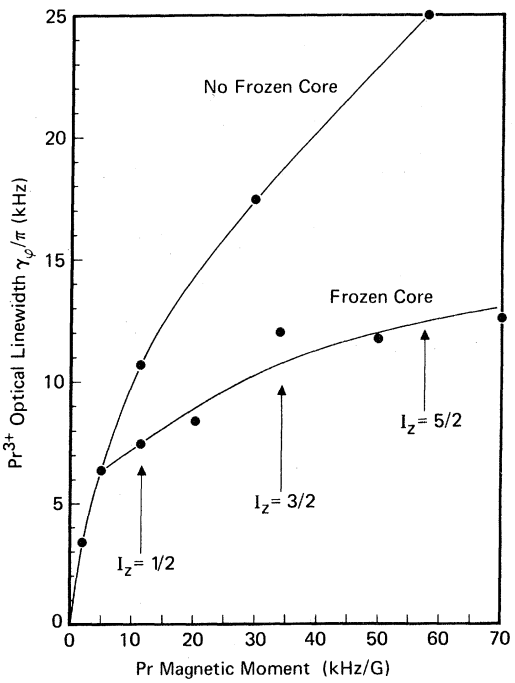

FIG. 5. The Pr^{3+} optical linewidth (γ_ϕ/π FWHM) vs the ^{141}Pr magnetic moment $\mu_z^{Pr} = \gamma_I I_z \hbar$ in units of kHz/G showing the linewidth reduction due to a frozen core where $T = 50$ μsec.

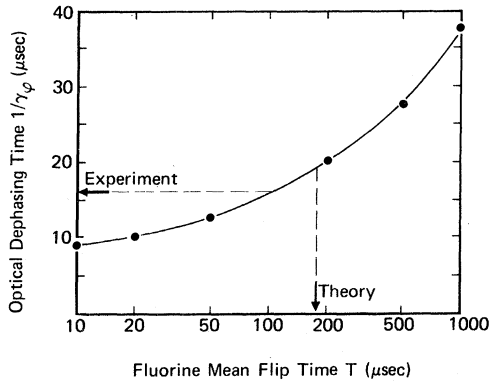

FIG. 6. The Pr^{3+} optical dephasing time $1/\gamma_\phi$ vs the fluorine mean flip time T. The optical FID result is $1/\gamma_\phi = 15.8$ μsec and the theoretical fluorine spin-flip time $T = 170$ μsec.

$T=170$ μsec, and with the aid of Fig. 6, we see that the Monte Carlo calculation predicts a dephasing time $1/\gamma_\phi=19$ μsec compared to the experimental value of 15.8 μsec. The agreement to an uncertainty of 15% is unusually good by the standards of previous theories.

C. Hole burning preparation and line shape studies

To include the effect of inhomogeneous broadening, we combine Eqs. (2.15), (3.1), and (3.7) and obtain for the optical FID signal

$$F(t)=\mathrm{Re}\left[\frac{1}{N}\sum_{j=1}^{N}[u_j(0)+iv_j(0)]e^{i\phi_j(t)}\right]=\frac{1}{N}\sum_{j=1}^{N}u_j(0)\cos\phi_j(t)-\frac{1}{N}\sum_{j=1}^{N}v_j(0)\sin\phi_j(t)\ , \tag{4.4}$$

given in terms of the preparation $u_j(0)$ and $v_j(0)$ at time $t=0$ and the phase $\phi_j(t)$ where the sum extends over all inhomogeneous environments expressed by the frequency shifts α_j.

Before evaluating Eq. (4.4), consider its reduction to the single packet case. In this circumstance, all ions of the packet are in phase at the beginning of the decay $t=0$ and have identical preparative factors so that Eq. (4.4) becomes

$$F(t)=\frac{u(0)}{N}\sum_{j=1}^{N}\cos\phi_j(t)\ -\frac{v(0)}{N}\sum_{j=1}^{N}\sin\phi_j(t)\ .$$

The sum over the sine terms tends to vanish since $\phi_j(t)$ has equal probability of being positive or negative, and Eq. (4.3) results,

$$F(t)=\frac{1}{N}\sum_{j=1}^{N}\cos\phi_j(t)\ ,$$

where we have set $u(0)=1$. For $LaF_3:Pr^{3+}$, since the maximum frequency jump due to a fluorine spin flip is 10 kHz, the FID sum (4.3) will have Fourier components limited by 10 kHz as well. Furthermore, since the cosine term has zero slope near $t=0$, the first 10 μsec of the decay will be highly *nonexponential.*

We will now see, however, that the effect of inhomogeneous broadening leads to near exponential behavior, in contrast to the single packet case. Thus, in Eq. (4.4) the term $\sum_j v_j(0)\sin\phi_j(t)$ no longer vanishes but is comparable in magnitude to $\sum_j u_j(0)\cos\phi_j(t)$. This follows since $v_j(0)$ and $\phi_j(t)$ are correlated and both are odd under frequency inversion so that their product is even. In addition, the frequencies contributing to $\phi_j(t)$ are no longer limited by the nearest-neighbor spin-flip value of 10 kHz, but are determined instead by the optical and magnetic *inhomogeneous* broadening. Even though the amplitude of the high-frequency components is reduced by their off-resonance response, high-frequency Fourier components can now appear in Eq. (4.4) producing a fast Gaussian response ($T_2^*\sim 100$ psec) near $t=0$ followed by a slower exponential decay ($1/\gamma_\phi=16$ μsec).

The line shape of the hole burned into the inhomogeneously broadened line of $LaF_3:Pr^{3+}$ is seen in Fig. 7, the linewidth being 10 kHz HWHM. This is a Monte Carlo calculation of the preparation at time $t=0$ where the line shapes correspond to the in-phase $(1/N)\sum_{j=1}^{N}u_j(0)$ and out-of-phase $(1/N)\sum_{j=1}^{N}v_j(0)$ contributions which are approximately Lorentzian. Thus, this case differs significantly from the non-Lorentzian behavior of a single packet.

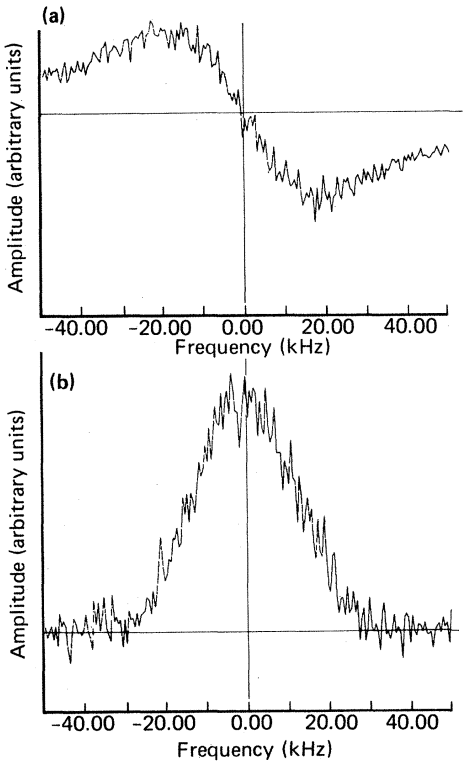

FIG. 7. The optical line shape function of Pr^{3+} during hole burning showing near Lorentzian behavior for the preparative step in terms of (a) the in-phase, $u(0)$, and (b) the out-of-phase, $v(0)$, components of the Bloch vector.

Similarly, Fig. 8 compares the observed[1] optical FID of the $^3H_4 \leftrightarrow {}^1D_2$ transition of $LaF_3:Pr^{3+}$, which is an exponential, with a Monte Carlo calculation that includes both the preparative and post-preparative periods. The calculated quantities $(1/N)\sum_j u_j(0)\cos\phi_j(t)$ and $(1/N)\times\sum_j v_j(0)\sin\phi_j(t)$, which assume a preparation time of 200 μsec and $I_z=\frac{3}{2}$, are plotted separately to show their exponential character. Alternatively, their difference as written in Eq. (4.4) leads to a partial cancellation and a numerical result which is far noisier and more difficult to interpret. Note that the two terms of Eq. (4.4) as plotted in Fig. 8 agree with the experimental data both in slope and shape, confirming once again the 10-kHz linewidth and the nearly Lorentzian line shape. Considering there are no free parameters in the theory, except for the vertical scale, the agreement is excellent.

We have so far compared both theory and experiment to an exponential decay law (Fig. 8), but in the Introduction we noted that $Pr^{3+}:LaF_3$ was an intermediate case, neither Lorentzian nor Gaussian in principle. In fact, both theory and experiment show partially Gaussian decay at short and long times, bracketing the intermediate exponential region. In Fig. 8, for example, for long times ($t > 16$ μsec) both theory and experiment decay faster than an exponential. For short times ($t < 2$ μsec) Gaussian-like behavior can be inferred from Fig. 7(b) which drops off faster than a Lorentzian for a detuning larger than 20 kHz. Future experiments with increased laser frequency and amplitude stability should clarify this complex decay behavior at short and long times.

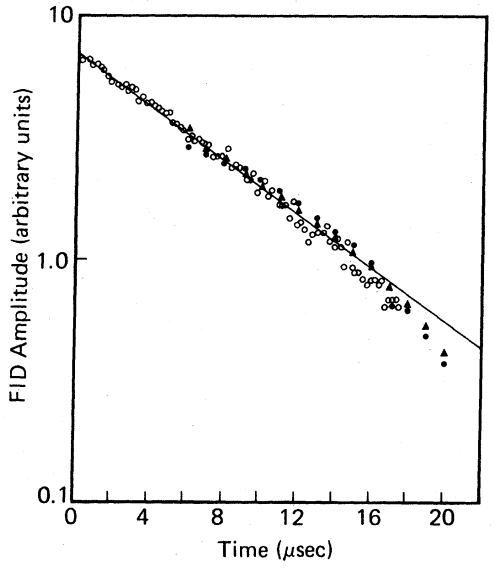

FIG. 8. Semilog plot of the FID signal versus time showing the experimental data: ○ and the Monte Carlo calculation in terms of the out-of-phase Δ: $\langle v\sin\phi\rangle$ and the in-phase ●: $\langle u\cos\phi\rangle$ components of the Bloch vector where $\chi=3$ kHz. The solid line corresponds to a dephasing time $1/\gamma_\phi=15.8$ μsec (linewidth: 10.1 kHz).

The rapid initial response near the time origin arising from the first order FID is not reproduced in these calculations because of the excessive computer time needed to integrate Eq. (3.1) over the full strain-broadened inhomogeneous linewidth of 5 GHz. Since this feature is well understood by previous analytic arguments,[3] the integration was restricted to $\Delta_j \leq 100$ kHz and consequently the calculated rise time (not shown in Fig. 8 because of the scale) is 5×10^4 times slower than the expected value $T_2^* = 100$ psec.

V. CONCLUSION

The Monte Carlo theory presented has demonstrated in a precise way that the 10-kHz optical homogeneous linewidth recently observed in $Pr^{3+}:LaF_3$ arises from the magnetic dipolar coupling of the Pr nucleus with the fluorine nuclei which undergo resonant spin flip-flops. The theory accurately predicts, via the variable frozen core argument, the single exponential decay function and gives the decay rate with no free parameters. Not only are the optical[1,2] linewidths predicted but those of nuclear quadrupole resonance[13,17,18] as well.

The Monte Carlo theory possesses several advantages over previous analytic theories. It bypasses an ambiguity present in applying the Klauder-Anderson model.[8] While the Klauder-Anderson parameter R is clearly defined when the spin flips are caused by spin-lattice relaxation, R has no clear meaning for the T_2 or resonant fluorine flip-flop process considered here.

Also, the Hu-Hartmann theory contains implicitly a spatial integral which cannot be evaluated for our system (Appendix A), so that this theory does not apply to $Pr^{3+}:LaF_3$ either.

Lastly, we have studied numerically nonlinear solutions of the Bloch equations, in the presence of stochastic phase and frequency fluctuations. Few, if any, analytic solutions to this general problem have been given and we suggest that the Monte Carlo method may have similar applications in gas collision theory as well as other line broadening problems in the solid state.

ACKNOWLEDGMENTS

We are indebted to L. E. Erickson for informing us of his unpublished results, the NQR inhomogeneous linewidth of $LaF_3:Pr^{3+}$ and its dependence on the

static external magnetic field. We also benefited from the preprint[14] of R. M. Macfarlane and R. M. Shelby. This work was supported in part by the U.S. Office of Naval Research.

APPENDIX: COMPARISON WITH HU-HARTMANN THEORY

An examination of the sudden jump theory of Hu and Hartmann[9] reveals the assumption of a lattice which is continuous rather than discrete. The implication of this assumption and its limits of validity are discussed in this section.

In the Monte Carlo calculation, the linewidth is dominated by the nearest neighbors while in the Hu-Hartmann theory there are no nearest neighbors since the B spins can be infinitesimally close to the A spins. We show that the Hu-Hartmann derivation may be valid for the case of large magnetic moments encountered in electron spin resonance, but fails for the nuclear spin case of Pr^{3+}:LaF_3. Their approximation lies in the spatial integral, their Eq. (2.10),

$$F(\tau)=\exp\left[n\mathfrak{a}\left\langle 1-\exp\left[i\omega_{\alpha\beta}\int_0^\tau h(t)\,dt\right]\right\rangle\right] . \tag{A1}$$

The brackets $\langle\ \rangle$ represent a spatial average defined in their Eq. (2.8), and

$$\omega_{\alpha\beta}\equiv\frac{2\mu_A\mu_B}{\hbar}\frac{(1-3\cos^2\theta_{\alpha\beta})}{r_{\alpha\beta}^3} . \tag{A2}$$

We make their approximation explicit by defining the variable

$$C\equiv\frac{2\mu_A\mu_B}{\hbar}(1-3\cos^2\theta)\int_0^\tau h(t)\,dt$$

so that the above expression becomes

$$F(\tau)=\exp\left[n\mathfrak{a}2\pi\int_0^\pi\sin\theta\,d\theta\int_{r_{\min}}^{r_{\max}}r^2dr\,(1-e^{iC/r^3})\right] . \tag{A3}$$

Klauder and Anderson[8] have examined a similar integral and point out that although it is always valid to replace $r_{\max}$ by ∞, $r_{\min}$ may be replaced by zero only in certain circumstances. Retaining $r_{\min}$ in the integral over r we find

$$F(\tau)=\exp\left[n2\pi\mathfrak{a}\int_0^\pi\sin\theta\,d\theta\times\left[\frac{C}{3}\int_0^{C/r_{\min}^3}\frac{du}{u^2}(1-\cos u)\right]\right] \tag{A4}$$

The upper limit of integration has a physical meaning:

$$\frac{C}{r_{\min}^3}=2\pi\nu_{\max}\int_0^\tau h(t)\,dt , \tag{A5}$$

where

$$\nu_{\max}\equiv\frac{1}{2\pi}\frac{2\mu_A\mu_B}{\hbar r_{\min}^3}(1-3\cos^2\theta) ,$$

is just the frequency jump due to the flipping of the nearest (or most strongly coupled) neighbor. The dimensionless integral

$$\int_0^x(1-\cos u)\frac{du}{u^2}$$

approaches $\pi/2$ for $x>2\pi$, but at small x is linear in x. Note that the integral in Eq. (A5) has dimensions of time and is always less than the duration of the experiment, Δt. The Hu-Hartmann theory assumes that $r_{\min}=0$, and that the radial integral reduces to $\pi C/6$, whereupon the remaining integration can be easily performed. We have shown, however, that this is true only when

$$\nu_{\max}\Delta t>1 . \tag{A6}$$

When $\nu_{\max}\Delta t<1$, the radial integral is a linear function of $\nu_{\max}\Delta t$ and therefore depends on the crystal structure via the nearest-neighbor interaction so that $F(\tau)$ in Eq. (A4) can no longer be integrated analytically. For electron spin resonance, where $\nu_{\max}\gg 1$ MHz and $\tau>1$ μsec, this condition is easily satisfied. For the optical dephasing of Pr^{3+}:LaF_3, where $\nu_{\max}$ is limited by the frozen core effect to 10 kHz and $\Delta t\sim 10$ μsec, it is always violated.[27]

For systems that satisfy this condition more closely than Pr^{3+}:LaF_3 we find the power series technique described in their Eq. (2.15) will fail after a certain number terms, depending on the size of $\nu_{\max}\Delta t$.

---

*Present address: Bell Telephone Laboratories, Holmdel, N.J. 07733.

†Present address: Dept. of Phys., Stanford University, Stanford, Cal. 94305.

[1]R. G. DeVoe, A. Szabo, S. C. Rand, and R. G. Brewer, Phys. Rev. Lett. 42, 1560 (1979).

[2]S. C. Rand, A. Wokaun, R. G. DeVoe, and R. G. Brewer, Phys. Rev. Lett. 43, 1868 (1979).

[3]R. G. DeVoe and R. G. Brewer, Phys. Rev. Lett. 40, 862 (1978); Phys. Rev. A 20, 2449 (1979).

[4]P. W. Anderson and P. R. Weiss, Rev. Mod. Phys. 25, 269 (1953).

[5]R. Kubo, in *Fluctuation, Relaxation and Resonance in Magnetic Systems,* edited by D. ter Haar (Oliver and Boyd Ltd., Edinburgh, 1962), p. 23.
[6]B. Herzog and E. L. Hahn, Phys. Rev. 103, 148 (1956).
[7]W. B. Mims, Phys. Rev. 168, 370 (1968).
[8]J. R. Klauder and P. W. Anderson, Phys. Rev. 125, 912 (1962).
[9]P. Hu and S. R. Hartmann, Phys. Rev. B 9, 1 (1974).
[10]A. Zalkin, D. H. Templeton, and T. E. Hopkins, Inorg. Chem. 5, 1466 (1966).
[11]A. Abragam, *Principles of Nuclear Magnetism* (Oxford University Press, Oxford, 1961).
[12]T. P. Das and E. L. Hahn, *Nuclear Quadrupole Resonance Spectroscopy* (Academic, New York, 1958).
[13]L. E. Erickson, Opt. Commun. 21, 147 (1977).
[14]R. M. Macfarlane and R. M. Shelby, Opt. Lett. 6, 96 (1981).
[15]J. H. Van Vleck, Phys. Rev. 74, 1169 (1948).
[16]N. Laurance, E. C. McIrvine, and J. Lambe, J. Phys. Chem. Solids 23, 515 (1962).
[17]L. E. Erickson, Phys. Rev. B 16, 4731 (1977).
[18]R. M. Shelby, C. S. Yannoni, and R. M. Macfarlane, Phys. Rev. Lett. 41, 1739 (1978).
[19]L. E. Erickson (private communication).
[20]A. Abragam and K. Kambe, Phys. Rev. 91, 894 (1953).
[21]W. B. Mims, in *Electron Paramagnetic Resonance,* edited by S. Geschwind (Plenum, New York, 1972), p. 291.
[22]M. A. Telplov, Zh. Eksp. Teor. Fiz. 53, 1520 (1967) [Sov. Phys. JETP 26, 872 (1968)]; B. Bleaney, Physica (Utrecht) 69, 317 (1973).
[23]K. Lee and A. Shir, Phys. Rev. Lett. 14, 1027 (1965); L. Shen, Phys. Rev. 172, 259 (1968).
[24]In our preliminary work, Ref. 1, a biexponential decay was observed at a static magnetic field of 19 G, whereas, in the earth's field or at 76 G or higher a single exponential was detected. More recently, with improved laser frequency stability, only single exponential decays have been seen.
[25]N. Bloembergen, Physica (Utrecht) 15, 386 (1949).
[26]I. J. Lowe and S. Gade, Phys. Rev. 156, 817 (1967).
[27]In Ref. 18, Shelby *et al.* observe an optically detected echo of a Pr^{3+} quadrupole transition in LaF_3 and attempt to fit their echo envelope function to Eq. (5.7) of the Hu-Hartmann (HH) theory (Ref. 9). In view of our discussion, the HH theory does not apply to this case and the apparent fit achieved is invalid. Furthermore, the numerical values of the parameters chosen,[18] $\Delta\omega_{1/2}=50$ kHz and $W=\frac{1}{17}$ μsec^{-1}, are inappropriate.